Preparation of Horseradish Peroxidase Modified Gold Nanoparticle/Coiled Carbon Nanotube Nanocomposite and its application for bromate and nitrite determination

Yucen Yao[1, 3!], Chunxiao Yin[1,!], Shiguan Xu[1], Meng Jiang[1], Lin Zhu[1], Ruyi Zou[2,], Wei Sun[1,*]*

[1] Key Laboratory of Water Pollution Treatment and Resource Rouse of Hainan Province, Key Laboratory of Functional Materials and Photoelectrochemistry of Haikou, College of Chemistry and Chemical Engineering, Hainan Normal University, Haikou 571158, P. R. China,
[2] Jiangxi Province Key Laboratory of Polymer Preparation and Processing, Shangrao Normal University, Shangrao 334001, P. R. China
[3] College of Chemical and Environmental Engineering, Chongqing University of Arts and Sciences, Chongqing 402160, P. R. China
[!]Co-first authors of the article
[*]E-mail: zuory2005@163.com, sunwei@hainnu.edu.cn

In this paper gold nanoparticles (AuNPs) were electrodeposited on the coiled carbon nanotubes (CCNTs) modified carbon ionic liquid electrode (CILE), and horseradish peroxidase (HRP) was fixed on the modified electrode by using Nafion film to get the modified electrode. HRP immobilized with AuNPs-CCNTs composite still retained the biostructure and direct electrochemistry of Nafion/HRP/AuNPs-CCNTs/CILE showed a quasi-reversible electrochemical behavior. Electrocatalysis to $KBrO_3$ and $NaNO_2$ were further checked with the apparent heterogeneous electron transfer rate constant (ks), the charge transfer coefficient (α) and the Michaelis-Menten constants (K_M^{app}) calculated. The linear detection range for $KBrO_3$ concentration was from 0.5 to 10.0 mmol·L^{-1} with a detection limit of 0.16 mmol·L^{-1}. And for $NaNO_2$, the current response showed two linear sections in the concentration range from 0.1 to 0.7 mmol·L^{-1} and 0.9 to 3.0 mmol·L^{-1} with low detection limit of 0.03 mmol·L^{-1}. The sensor was used for the real water samples analysis with high recovery, demonstrating the practical applications.

1. INTRODUCTION

Bromate and nitrite have been classified as 2A and 2B carcinogen by the International Agency for Research on Cancer (IARC) [1,2]. Due to the presence of nitrite in vegetables and pickled foods [3], and the abuse of food additives containing potassium bromate [4], nitrite and bromate present in foods are hazardous to human health if ingested. Therefore, accurate determination of trace amounts of nitrite

and bromate is of great significance in practical usages. For this purpose, various analytical methods such as ion chromatography [5, 6], spectrophotometry [7] and capillary electrophoresis [8] were devised. However, it's still challenging to devise new method with high detection sensitivity and extensive working range.

Biosensors with heme (coenzyme group) as the electroactive center can provide an electrochemical method for detecting nitrite and bromate due to their features such as the miniaturized instruments, wide analytical range, high sensitivity and selectivity [9]. For example, Palanisam et al. designed the biosensor based on direct electrochemistry of hemoglobin with a detection limit of 33 nM for bromate [10]. Liu et al. developed a nitrite sensor with a detection limit of 0.12 μM [11]. Horseradish peroxidase (HRP) contains heme as a prosthetic group, which is a suitable enzyme for building third-generation biosensors. It has been proven to exhibit electrocatalytic activity and quantitative analysis of bromate and nitrite. Gold nanoparticles (AuNPs) are excellent electrocatalyst with stable chemical properties, good electrical conductivity and excellent biocompatibility, which have been reported for the development of novel chemical and biological sensors [12, 13]. Also AuNPs had been loaded with other nanomaterials such as graphene nanoribbon [14] and biomass carbon [15] for electrochemical applications with high efficiency and stability. As a novel carbonaceous material, the helically coiled carbon nanotubes (CCNTs) were first discovered by Zhang et al [16]. CCNTs have attracted widespread attentions due to the excellent mechanical, optical and electronic properties, which are suitable for use as a catalyst carrier to enhance the catalytic activity with unique helical structure and exceptional properties [17]. Ma et al. prepared ZnO/N-CCNTs as a photocatalyst for degradation of organic pollutants [18]. Wang et al. reported Pd/CCNTs for electrooxidation of ethanol [19]. Therefore, the CCNTs-based composites have been used in various research fields.

In this work, we presented a CCNTs-AuNPs composite layer to promote the electrocatalytic activity of HRP, which was present on a carbon ionic liquid electrode (CILE) to construct enzyme sensor (Nafion/HRP/AuNPs-CCNTs/CILE). The process of fabricating the modified electrode and the application of this electrode for the detection of nitrite and bromate are shown in Scheme 1.
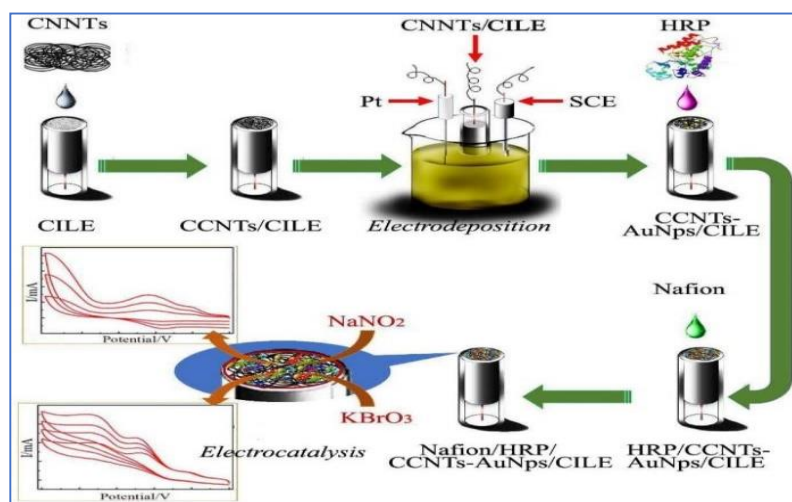
Scheme 1. Schematic illustration of the fabrication process and electrocatalysis of Nafion/HRP/AuNPs-CCNTs/CILE.

2. EXPERIMENTAL SECTION

2.1. Reagents

HRP (MW. 40000, Sinopharm Chem. Reagent Co., China), CCNTs (Nanjing XFNANO Materials Tech. Co. Ltd., China), graphite powder (average particle size 30 μm, Shanghai Colloid Chem. Co. Ltd., China), 1-hexylpyridinium hexafluorophosphate (HPPF$_6$, Lanzhou Yulu Fine Chem. Co. Ltd., China), chloroauric acid (HAuCl$_4$, Shanghai Chem. Plant, China), KBrO$_3$ and NaNO$_2$ (Shanghai Aladdin Reagent Co. Ltd., China) were directly used. 0.1 mol·L^{-1} PBS was prepared as the supporting electrolyte and ultra-pure water (Milli-Q IQ-7000, USA) was used in all the experiments. Before the experiment was performed, high-purity nitrogen gas must be introduced into PBS for 30 minutes to eliminate the interference of oxygen dissolved in the solution.

2.2. Apparatus

Cyclic voltammetry (CV) and electrochemical impedance spectroscopy (EIS) were recorded by three-electrode system on a CHI 660D electrochemical workstation (Shanghai CH Instruments, China). The as-prepared electrodes were served as working electrode with a saturated calomel electrode (SCE) and a platinum wire as reference electrode and counter electrode. Scanning electron microscopy (SEM) was conducted with a JEOL JEM-2010HT scanning electron microscope (Japan). Fourier transform infrared (FT-IR) spectrum and ultraviolet-visible (UV-Vis) absorption spectrum were on Nicolet 6700 FT-IR spectrometer (Thermo Fisher Scientific Inc., USA) and TU1901 double-beam UV-visible spectrophotometer (Beijing Purkinje General Instrument Co., Ltd., China).

### 2.3. Fabrication of Nafion/HRP/AuNPs-CCNTs/CILE

Based on reference [20], CILE was fabricated by using the mixture of graphite powder and HPPF$_6$ into a glass electrode tube (Φ=4 mm), which was polished to a mirror-like surface before use. Thereafter, CILE was modified with 6.0 μL of 0.5 mg·mL^{-1} CCNTs suspension and dried to obtain CCNTs/CILE. Then CCNTs/CILE was placed in 1.0 mmol·L^{-1} HAuCl$_4$ solution to prepare AuNPs-CCNTs/CILE by potentiostatic electrodeposition at -0.3 V for 50 s. Subsequently, 8.0 μL of 15.0 mg·mL^{-1} HRP solution and 6.0 μL of 0.5% Nafion solution were dropped onto the electrode in turn and dried after each step to obtain the modified electrode (Nafion/HRP/AuNPs-CCNTs/CILE). Referring to the above steps, other modified electrodes including Nafion/CILE, Nafion/HRP/CILE and Nafion/HRP/AuNPs-CCNTs/CILE were prepared for experimental comparison.

3. RESULTS AND DISCUSSION

3.1. SEM images

SEM images show that CCNTs have a typical three-dimensional helical structure similar to spring (Fig. 1 A and B) with pitch size of 100±10 nm. Fig. 1 C and D show that AuNPs are dispersed on

the spiral structure of CCNTs in a messy manner to form AuNPs-CCNTs composites. The circles in Fig. 1 C and D labelled several clusters of AuNPs on the surface of CCNTs, which were formed by directly electrodeposition.
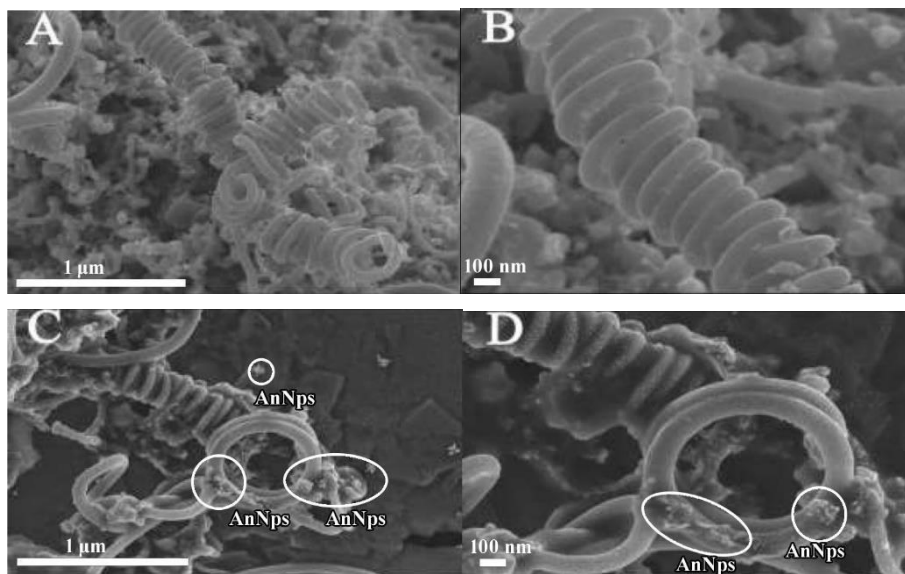
Figure 1. SEM images of CCNTs (A, B) and AuNPs-CCNTs (C, D)

3.2. Spectroscopic investigations

Spectroscopic characteristics of proteins can be elucidated from their secondary structure. The conformational change of the porphyrin in HRP will cause the shift of the Soret band in the UV-Vis region. Fig. 2 A depicts the UV-Vis spectrum of HRP (curve a) and HRP/AuNPs-CCNTs mixture (curve b) in pH 3.0 PBS, which exhibits two identical Soret bands at 403 nm [20]. Therefore, the biological structure of HRP after mixed with AuNPs-CCNTs composite remains unchanged. Further, the structure of polypeptide chain of HRP was analyzed by FT-IR with the spectra depicted in Fig. 2 B. The amide I and amide II bands of the pure HRP appear at 1650 cm^{-1} and 1540 cm^{-1} (curve a) [21], which are in consistent with that of HRP/AuNPs-CCNTs (curve b). Therefore, HRP is not denatured after mixing with the AuNPs-CCNTs composite, and all spectroscopic investigations prove that composite film has good biocompatibility.
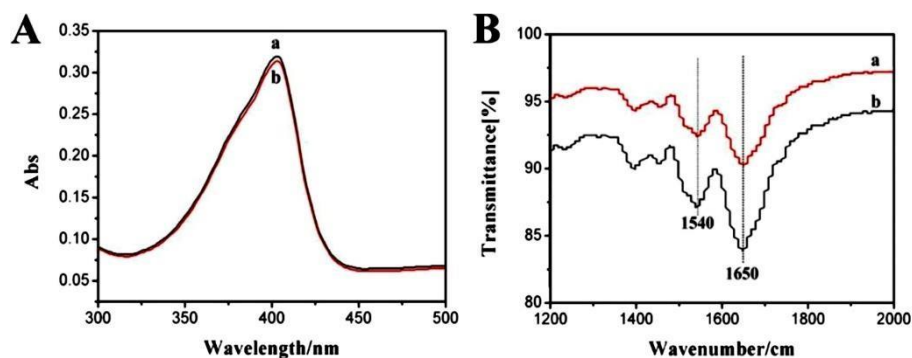
Figure 2. (A) UV-Vis absorption spectra of HRP (a) and HRP/AuNPs-CCNTs (b) in pH 3.0 buffer; (B) FT-IR spectra of HRP (a) and HRP/AuNPs-CCNTs composite (b).

3.3. Electrochemical investigations

CV responses of different electrodes were investigated at scan rate of 0.1 V·s^{-1} in PBS (pH 3.0) with curves shown in Fig. 3 A. No redox peaks were observed at CILE or Nafion/CILE (curves a and b), which proved the absence of electroactive substances on the electrode surface. While the redox peaks are significant at Nafion/HRP/CILE, Nafion/HRP/CCNTs/CILE and Nafion/HRP/AuNPs-CCNTs/CILE (curves c, d and e). Moreover, due to the different HRP modified electrodes, the intensity of the redox peak currents of each electrode is different. Especially for Nafion/HRP/AuNPs-CCNTs/CILE, the largest peak currents indicated that AuNPs-CCNTs composite has the best ability to promote the direct electron transfer of HRP due to the synergistic effects including high conductivity and specific surface area. From curve e, the potentials of the oxidation and the reduction peak are -0.231 V (Epc) and -0.126 (Epa), respectively, and the peak-to-peak difference (ΔEp) is 105 mV with the formal peak potential (E$^{o'}$) as -0.179 V (vs. SCE). The ratio of oxidation peak current to reduction current (Ipc/Ipa) is close to 1, indicating that the redox reaction of HRP is an approximately reversible electrochemical reaction process.

EIS experiments are measured in the frequency range between 0.01 Hz and 100 KHz, which can characterize the electrochemical nature of electrode materials and monitor the impedance changes related to the electrode/electrolyte interface at each modification step. It is generally accepted that the diameter in the high-frequency region of the Nyquist plot is a measure of the charge transfer resistance (Rct). Fig. 3 B shows the Nyquist plots of CILE, Nafion/CILE, Nafion/HRP/CILE, Nafion/HRP/CCNTs/CILE and Nafion/HRP/AuNPs-CCNTs/CILE with the Rct values as 38.8 Ω, 23.9 Ω, 183.4 Ω, 103.6 Ω and 58.1 Ω, respectively. The results prove that high conductive AuNPs-CCNTs composite improves the interfacial charge transfer efficiency with Nafion and HRP increased the interfacial resistance.

Electrochemical behaviors of Nafion/HRP/AuNPs-CCNTs/CILE were checked at different pH buffer by CV. As shown in Fig. 4 A, the redox peak potentials are negatively shifted with the increment of pH value of PBS, indicating the protons in the electrode reaction. The formal peak potential (E$^{o'}$) has a good linear relationship with pH and the equation is E$^{o'}$ (V) = -0.0573 pH + 0.0361 (n=6, γ=0.992). The slope of -57.3 mV·pH^{-1} is almost the same as the theoretical value (-59.0 mV·pH^{-1}) of the reversible system at 25°C, indicating that same electron and proton were involved in the redox reaction of HRP

with the equation as HRP Fe (III) + H$^+$+ e $\rightleftharpoons$ HRP Fe(II) [22]. Moreover, the maximum peak current appeared at pH 3.0, which was used for all experiments.
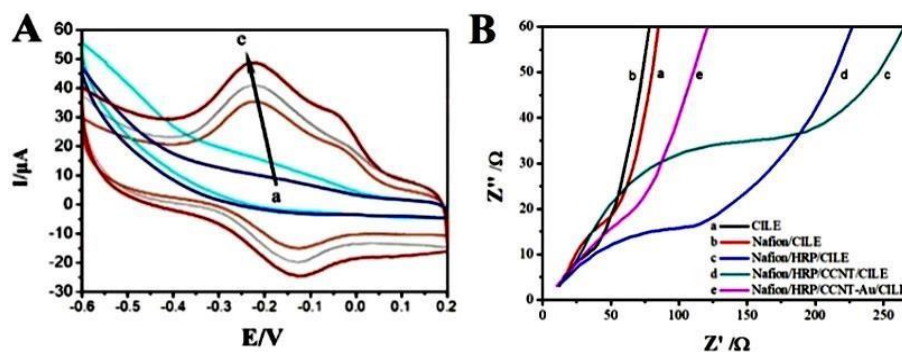
Figure 3. (A) Cyclic voltammograms and (B) Nyquist plots of different electrodes in pH 3.0 PBS. Electrodes: CILE (a), Nafion/CILE (b), Nafion/HRP/CILE (c), Nafion/HRP/CCNTs/CILE (d), Nafion/HRP/AuNPs-CCNTs/CILE (e).
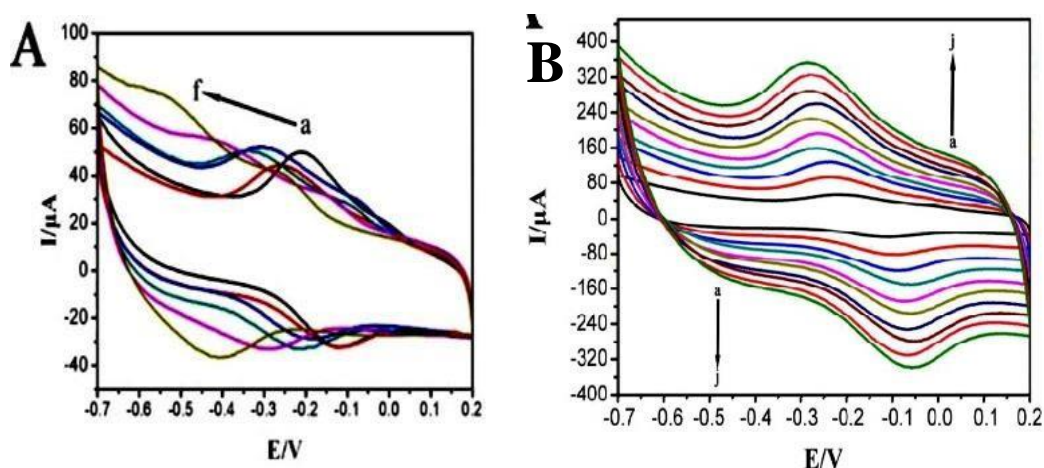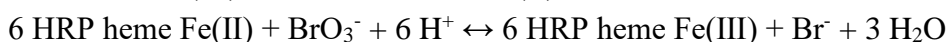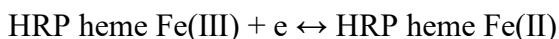

Figure 4. (A) Influence of buffer pH on Nafion/HRP/AuNPs-CCNTs/CILE at scan rate of 0.1 V·s^{-1} (a to f: 3.0, 4.0, 5.0, 6.0, 7.0, 8.0); (B) CVs of Nafion/HRP/AuNPs-CCNTs/CILE at different scan rates (from a to j as 100, 200, 300, 400, 500, 600, 700, 800, 900, 1000 mV·s^{-1}) in pH 3.0 buffer

The relationship between scan rate and direct electrochemical data of Nafion/HRP/AuNPs-CCNTs/CILE was discussed by CV (Fig. 4B). A pair of redox peaks originated form HRP appeared from 0.1 to 1.0 V·s^{-1} with the redox peak currents of HRP increased simultaneously. Meanwhile the redox peak potentials showed a small shift and ΔEp became slightly enlarged. A good linear relationship between the redox peak current (Ip) and scan rate is presented with the equations as Ipc (μA) = -58.96v (V·s^{-1}) + 4.04 (n = 10, γ = 0.990) and Ipa (μA) = -77.15v (V·s^{-1}) -16.09 (n=10, γ = 0.995). Moreover, Ep and ln$v$ also have linear relationships with their regression equations as Epc (V) = -0.080 ln$v$ (V·s^{-1}) - 0.291 (n=6, γ=0.992) and Epa (V) = 0.0571 ln$v$ (V·s^{-1}) 0.050 (n=6, γ=0.993). According to Laviron's theory [23], the electron transfer coefficient (α) is obtained as 0.43, which is close to the reported value of 0.42 [24]. The number of electrons transferred (n) and heterogeneous electron transfer rate constant (k_s) are calculated as 1.26 and 1.17 s^{-1}. The k_s value is higher than the reported value of 1.01 s^{-1} [25], proved that Nafion/HRP/AuNPs-CCNTs/CILE made the electron exchange faster.

3.4. Electrocatalysis

The electrocatalytic reduction of $KBrO_3$ by Nafion/HRP/AuNPs-CCNTs/CILE was investigated and Fig. 5 A shows the CV responses in $KBrO_3$ solution. With the addition of $KBrO_3$ in the buffer solution, the reduction peak current at -0.233 V was markedly increased with the oxidation peak current decreased. The mechanism for the catalytic reduction of $KBrO_3$ with HRP can be approximately described by the following equations [26]:

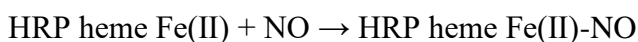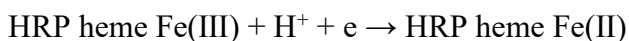HRP heme Fe(III) + e $\leftrightarrow$ HRP heme Fe(II)

6 HRP heme Fe(II) + BrO_3^- + 6 H^+ $\leftrightarrow$ 6 HRP heme Fe(III) + Br^- + 3 H_2O

The calibration plot depicts that the reduction peak currents are linear over the $KBrO_3$ concentration from 0.5 to 10.0 mmol·L^{-1} (inset of Fig. 5 A) with the regression equation as Ipc(μA) =16.49 C (mmol·L^{-1}) + 44.54 (n=11, γ=0.993) and the limit of detection (LOD) as 0.16 mmol·L^{-1} (3σ). When the C_{KBrO_3} exceeds 10.0 mmol·L^{-1}, the Ipc almost remained constant, implying a typical feature of Michaelis–Menten response. According to the Lineweaver–Burk equation [27], the Michaelis–Menten constant (K_M^{app}) of the electrocatalytic reaction to $KBrO_3$ is calculated to be 6.08 mmol·L^{-1}.
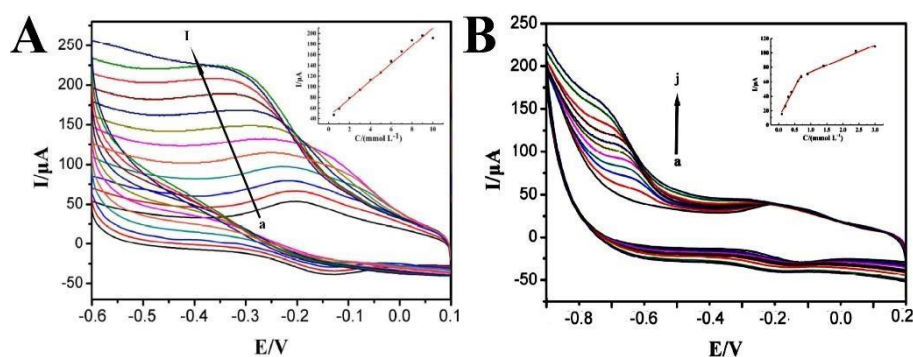
Figure 5. CVs of Nafion/HRP/AuNPs-CCNTs/CILE with different concentration of (A) $KBrO_3$ (a to l: 0.5, 1.0, 2.0, 3.0, 4.0, 5.0, 6.0, 7.0, 8.0, 9.0, 10.0, 12.0 mmol·L^{-1}; inset is the linear relationship of cathodic current versus $KBrO_3$ concentration) and (B) $NaNO_2$ (a to j: 0.1, 0.2, 0.3, 0.4, 0.6, 0.7, 0.9, 1.4, 2.4, 3.0 mmol·L^{-1}; inset is the linear relationship of cathodic current versus $NaNO_2$ concentration).

As depicted in Fig. 5 B, the electrocatalysis of Nafion/HRP/AuNPs-CCNTs/CILE to $NaNO_2$ was also examined with a new peak appeared at -0.623 V. It is generally believed that the peak was caused by the reduction reaction of the complex formed by the binding of NO to heme under mildly acidic conditions, and the NO was derived from the disproportionation reaction of nitrite [28]. The mechanism of electrocatalytic reduction of NO at HRP/AuNPs-CCNTs film is suggested to be the following equations [29]:

3 NO_2^-+$H_2O$$\leftrightarrow$2 NO (aq)+$NO_3^-$+2 OH^-

HRP heme Fe(III) + H^+ + e $\rightarrow$ HRP heme Fe(II)

HRP heme Fe(II) + NO $\rightarrow$ HRP heme Fe(II)-NO

HRP heme Fe(II)-NO+ H^+ +e $\rightarrow$ HRP heme Fe(II) + product + H_2O

Similarly, a linear relationship between C_{NaNO_2} and Ipc can be obtained with two sections from 0.1 to 0.7 mmol·L^{-1} and 0.9 to 3.0 mmol·L^{-1}, respectively. The corresponding linear regression equations were calculated as Ipc(μA) = 84.85 C (mmol·L^{-1}) +992 (n=6, γ=0.991) and Ipc(μA) = 18.53 C (mmol·L^{-1}) + 55.17 (n=4, γ=0.992). The LOD is got as 0.03 mmol·L^{-1} (3σ) with K_M^{app} as 7.66 mmol·L^{-1}. In table 1 the comparison of different modified electrodes for NaNO$_2$ detection were summarized, and the results showed that this method had excellent linear range and detection limit.

Table .1 Comparison of different modified electrodes a for NaNO$_2$ detection

Modified electrodes	Linear range (mmol L^{-1})	Detection limit (mmolL^{-1})	Reference
Nafion/HRP/WS$_2$/CILE	1.5-4.0	0.20	[30]
Nafion/Hb/Co$_3$O$_4$-CNF/CILE	1.0–12.0	0.33	[31]
Nafion/Hb/Au/ZIF-8/CILE	0.1-0.8	0.03	[32]
Nafion/HRP/AuNPs-CCNTs/CILE	0.1-0.7, 0.9-3.0	0.03	This work

3.5. Practicability, stability and reproducibility

The practicability of Nafion/HRP/AuNPs-CCNTs/CILE was tested by detecting the content of BrO$_3^-$ and NO$_2^-$ in barreled mineral water samples (Haikou Coconut Water Co. Ltd., China). The recovery was estimated by standard addition method with results listed in table 2. The recovery and relative standard deviation (RSD) indicate that the proposed biosensor is feasible for the real sample analysis.

Table 2. Analysis results of KBrO$_3$ and NaNO$_2$ in a real water sample (n = 5)

Sample	Detected (mmol·L^{-1})	Added (mmol·L^{-1})	Found (mmol·L^{-1})	Recovery (%)	RSD (%)
		2.00	1.98	98.79	1.26
KBrO$_3$	0	6.00	5.87	97.75	2.36
		10.0	9.87	98.72	1.47
		0.40	0.38	95.85	3.17
NaNO$_2$	0	1.20	1.17	97.82	2.49
		2.00	1.98	98.96	1.26

Cyclic voltammetric responses of Nafion/HRP/AuNPs-CCNTs/CILE in PBS (pH 3.0) at room temperature displayed no significant change after 50 cycles, and the peak current retained 95.1% of the

original value after stored at 4 ℃ for 30 days. Five independently modified electrodes were used to test KBrO$_3$ (5.0 mmol·L^{-1}) and NaNO$_2$ (0.5 mmol·L^{-1}) with RSD of 1.3% and 1.6%, respectively. Therefore, Nafion/HRP/CCNTs-AuNPs/CILE had good stability and reproducibility.

4. CONCLUSION

A new HRP modified electrode (Nafion/HRP/AuNPs-CCNTs/CILE) was designed and fabricated with its electrocatalytic activity checked in detail. Due to the good biocompatibility of AuNPs-CCNTs nanocomposite, the biostructure of HRP on the electrode was maintained, which ensured the catalytic effect of enzyme electrode. Furthermore, the electrode showed excellent electrocatalytic behaviors to the reduction of KBrO$_3$ and NaNO$_2$. Therefore, AuNPs-CCNTs composites were suitable for the construction of third-generation enzyme sensors.

References

1. Y. Hung, W. Verbeke, T. De Kok, *Food Control.*,60(2016) 690.
2. M. Moore, T. Chen, *Toxicology*, 221(2006)190.
3. Z .Wang, Y. Shao, *Food Microbiol.*, 72(2018)185.
4. S. Kuo, Y. Li, Y. Cheng, W. Lee J. Cheng K. Cheng, *Mol. Med. Rep.*, 18(2018)4700.
5. E. Salhi, U. Von Gunten, *Water Res.*, 33(1999)3239.
6. L. Jackson, R. Joyce, M. Laikhtman, P. Jackson, *J. Chromatogr. A.*, 829(1998)187.
7. A. Kazemzadeh, A. Ensafi, *Microchem. J.,* 69(2001)61.
8. F. Della Betta, M. Siqueira, *J. Food Compos. Anal.*, 79(2019)63.
9. H. Liu, K. Guo, J. Lv, Y. Gao, C. Duan, L. Deng, Z. Zhu, *Sensor. Actuat. B:Chem.,* 238(2017)249.
10. S. Palanisamy, Y. Wang, S. Chen, B. Thirumalraj, B. Lou, *Microchim. Acta*,183(2016)1953.
11. H. Liu, C. Duan, C. Yang, W. Shen, F. Wang, Z. Zhu, *Sensor. Actuat. B:Chem.*, 218(2015)60.
12. M. Daniel, D.Astruc, *Chem. Rev.*, 104 (2004)293.
13. K. Saha, S. Agasti, C. Kim, X. Li, V. Rotello, *Chem. Rev.*, 112(2012)2739.
14. L.J. Yan, B. Shao, X. P. Zhang, Y.Y. Niu, W.D. Dang, H. Cheng, G.J. Li, W. Sun, *Curr. Anal. Chem.*, 17(2021)418.
15. H. Cheng, W.J. Weng, H. Xie, J. Liu, G.L. Luo, S.M. Huang, W.Sun, G.J. Li, *Microchem. J.*, 154(2020)104602.
16. X. B. Zhang, X. F. Zhang, D. Bernaerts, G. van Tendeloo, S. Amelinckx, J. van Landuyt, V. Ivanov, J. B. Nagy, P. Lambin, A. Lucas, *Europhys Lett.,* 27(1994)141.
17. R. Vijayan, A. Ghazinezami, S.Taklimi, M. Khan, D. Askari, *Compos. Part B: Eng.*, 156(2019) 28.
18. S. Ma, Q. Li, Z. Cai, Z. Ye, Y. Zhou, *Appl. Organometal Chem.*, 32(2018), e3966.
19. B. Wang, R. Cui, Z. Han, Y. Zhang, L. Wang, *Int. J. Electrochem. Sci.*, 14(2019)2265.
20. X.Q. Li, B. Shao, Y.X. Sun, B.X. Zhang, X.H. Wang, W. Sun, *Int. J. Electrochem. Sci*., 16 (2021) 210219.

21. D.M. Byler, H. Susi, *Biopolymers*, 241(2017)852.
22. W. Zheng, W. Chen, W. Weng, L. Liu, G. Li, J. Wang, W. Sun, *J. Iran Chem. Soc.*, 14(2017) 925.
23. E. Laviron, *J. Electroanal. Chem.*, 101 (1979)19.
24. A.K.M. Kafi, M. Naqshabandi, M.M.Yusoff, M.J. Crossley., *Enzyme Microb. Technol.,* 113 (2018) 67.
25. Y.Y. Niu, J.Liu, W.Chen, C.X Yin, W.J.Weng, X.Y. Li, X.L.Wang, G.J. Li, W. Sun, *Anal. Methods*, 10(2018)5297.
26. Y. Li, X. Lin, C. Jiang, *Electroanalysis*, 18(2006)2085.
27. R. A. Kamin, G.S. Wilson, *Anal. Chem.,* 52(1980)1198.
28. M. Barley, T. Meyer, *J. Am. Chem. Soc.*, 108(1986)5876.
29. F. Gomes, L. Maia, C. Cordas, C. Delerue-Matos, I. Moura, J. G. Moura, S. Morais, *Electroanalysis*, 30(2018) 2485.
30. Y.Y Niu, R.Y.Zou, H.A.Yones, X.B.Li, X.Y. Li, X.L.Niu, Y.Chen, P.Li, W.Sun, *J. Chin. Chem. Soc.*, 65 (2018)1127.
31. H.Xie, G.L.Luo, Y.Y.Niu, W.J.Weng, Y.Y.Zhao, Z.Q.Ling, C.X.Ruan, G.J.Li, W.Sun, *Mater. Sci. Eng. C.,* 107 (2020) 110209.
32. J. Liu, W.J. Weng, C. X. Yin, G.L. Luo, H. Xie, Y.Y. Niu, X.Y. Li, G.J. Li, Y. Xi, Y.T.Gong, S.Y. Zhang, W. Sun, *Int. J. Electrochem. Sci*., 14 (2019) 1310.